ISBN: 978-3-95450-234-9 ISSN: 2673-5504 doi:10.18429/JACoW-SRF2023-WEPWB048

GEOMETRY OPTIMIZATION FOR A QUADRUPOLE RESONATOR AT JEFFERSON LAB*

S. Bira, A-M. Valente-Feliciano, M. Ge
Thomas Jefferson National Accelerator Facility, Newport News, VA, USA
L. Vega Cid, W. Venturini Delsolaro, CERN, Geneva, Switzerland

Abstract

The quadrupole resonator (QPR) is a sample characterization tool to measure the RF properties of superconducting materials using the calorimetry method at different temperatures, magnetic fields, and frequencies. Such resonators are currently operating at CERN and HZB but suffer from Lorentz force detuning and modes overlapping, resulting in higher uncertainties in surface resistance measurement. Using the two CERN's QPR model iterations, the geometry was optimized via electromagnetic and mechanical simulations to eliminate these issues. The new QPR version was modeled for an increasing range of magnetic fields. The magnetic field is concentrated at the center of the sample to reduce the uncertainty in surface resistance measurements significantly. This paper discusses the QPR geometry optimization for the new version of QPR, which is now progressing toward fabrication.

INTRODUCTION

So far, almost all the superconducting accelerator cavities are generally made of bulk Niobium. High-performing Nb cavities have reached high accelerating gradients of ~50 MV/m on the beam axis, corresponding to a peak surface magnetic field of $B_c = 200$ mT, which is close to the fundamental limit of Niobium [1]. New materials such as Nb_3Sn, NbN, and MgB_2 that have higher critical temperatures and critical magnetic fields must be investigated to improve the performances of the accelerating cavities further. The deposition of elliptical cavities with these materials is often difficult and requires yet extensive development. Therefore, performing RF tests, specifically for the surface resistance measurement on flat samples, is essential. These tests must be realized with high-resolution surface resistance measurements in a large range of magnetic fields and operating temperatures. A quadrupole resonator is made to realize these measurements.

The schematic view of the resonator is shown in Fig. 1. It consists of four wire transmission lines related to a loop pair at the bottom end. All of these are fixed in the enclosed cylinder. The rod's top end is welded to the top of the cylinder. The length of the rods defines the fundamental frequency of the resonator. It is adjusted to λ/2 of the baseline operation frequency of 400 MHz. The sample is fixed at the bottom end of the cylinder, below the loops, where the magnetic field is maximum. The sample is welded to a niobium cylinder from the measuring chamber of the quadrupolar resonator [2, 3].

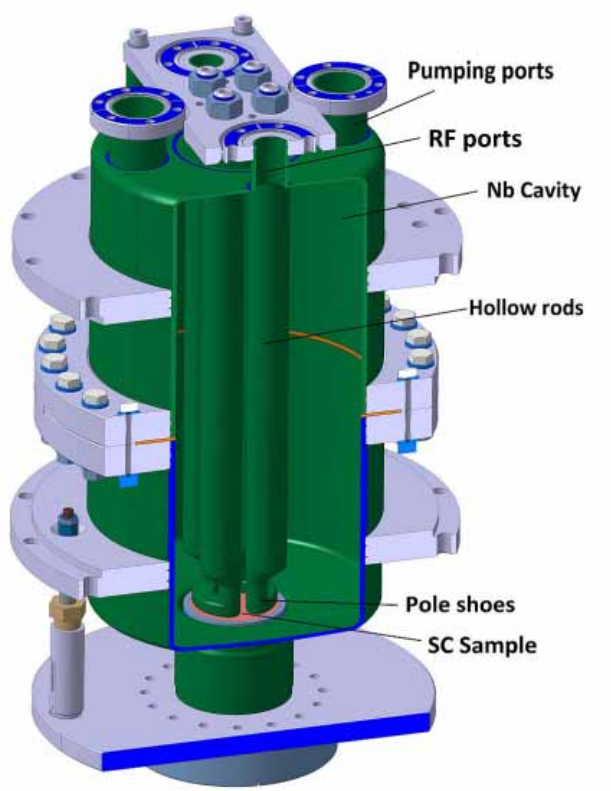

Figure 1: 3D view of the second quadrupole resonator at CERN [4].

The surface resistance is measured with a calorimetric compensation technique. Behind the sample, the heating element and thermocouples are fixed; the magnetic field is higher when heating at the center, and the thermocouples measure the temperatures (see Fig. 2). The measurement principle is straightforward; the sample is heated to a temperature of interest, $T_{interest}$. After the thermal equilibrium is established across the sample surface, RF power is applied, and the temperature of the sample increases. Decreasing the heating power to $T_{interest}$ allows us to determine the RF dissipated power on the sample. Assuming R_S is constant over the sample surface, it can be calculated with the following equation [5,6]:

$$R_S = \frac{2*(P_{DC1}-P_{DC2})}{\int_{Sample}|H|^2 dS} \quad (1)$$

* work supported by the U.S. Department of Energy, Office of Science, Office of Nuclear Physics under contract DE-AC05-06OR23177 with Jefferson Science Associates.
† bira@jlab.org

ISBN: 978-3-95450-234-9 ISSN: 2673-5504 doi:10.18429/JACoW-SRF2023-WEPWB048

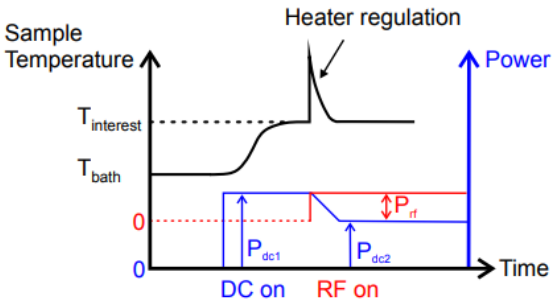

Figure 2: Schematic representation of the measurement principle of the QPR.

RF PARAMETERS

The main goal of the electromagnetic design of a quadrupole resonator is to get the highest possible magnetic field on the sample, which allows to get the best characterization of superconducting samples on a wide range of magnetic fields. The electromagnetic RF design is based on the evaluation of the following parameters as a function of the QPR geometry parameters [7]:

- $\Delta f = f_{quadrupole} - f_{dipole}$;

where f_{dipole} is the mode nearest to the fundamental mode of the QPR. This parameter should be higher than 5 MHz to avoid overlapping modes.

- B_{sample}/B_{peak};

where B_{peak} is the maximum surface magnetic field in the resonator, B_{sample}; is the maximum surface magnetic field on the sample. The higher the value of this ratio higher would be the range of the magnetic field for measurement.

- E_{peak}/B_{sample};

where E_{peak} is the maximum surface electric field in any surface quadrupole resonator. This ratio should be lowered to decrease the risk of field emission [8].

- $c = B_{peak}/\int_{Sample} B^2\, dS$;

where the $\int_{Sample} B^2\, dS$ is the integral magnetic field over the sample surface. This ratio should be higher to increase the concentration of the field on the sample.

- B_{edge}/B_{sample};

where B_{edge} is the magnetic field on the sample's edge. This ratio should be lower to minimize the heat on the coaxial gap.

- $\int_{Sample} B^2\, dS/U$;

The integral of the magnetic field on the sample surface is divided by the stored energy: this ratio should be higher to maximize the magnetic field illuminating the sample for the same stored energy.

The performance requirements are listed in Table 1. They were derived from the experience with CERN QPR 1 and 2.

Table 1: Requirements of the JLab QPR

Fields ratio	requirement
Δf	≥ 6 MHz
B_{sample}/B_{peak}	0.86
E_{peak}/B_{sample}	< 0.21 MV/m. mT
c	> 1000
B_{edge}/B_{sample}	< 0.1
$\int_{Sample} B^2\, dS/u$	> 70 mT^{2}J^{-1}

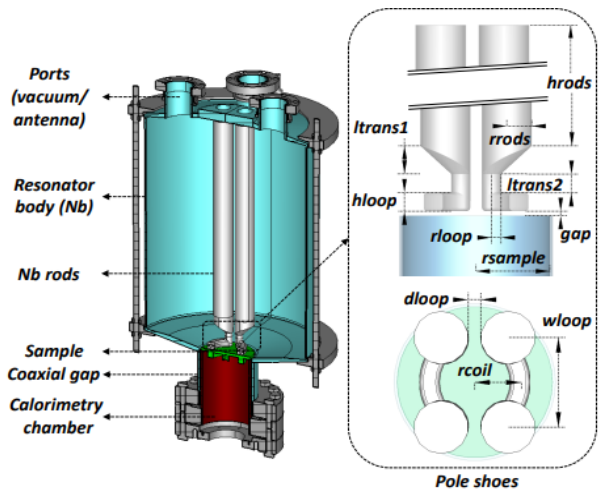

Figure 3: The parametrized model of the QPR [9].

SIMULATION

The optimization of the quadrupole resonator was performed in CST Microwave Studio using an adaptive tetrahedral mesh. Figure 3 shows a cross-sectional view of the QPR model and the main geometry parameters used for optimization. Each parameter was modified to study its effect on the distribution of electromagnetic field on the sample and the variation of RF figures of merit on some parameters is shown.

The simulation shows that E_{peak}/B_{sample} decreases with the increase of the radius of the rods (see Fig. 4), which can be explained by the fact that the increasing rod's radius allows the charge to spread over a large surface area. The variation of the magnetic field ratio on the sample is small, with respect to the variation of the radius of the rods. The large radius of the rods also lowers the mechanical vibration frequency due to the environment. On the other hand, the width of the rods has a significant effect on the overlapping modes; as shown in Fig. 5, the variation of Δf is estimated to be 1 MHz/mm.

ISBN: 978-3-95450-234-9 ISSN: 2673-5504 doi:10.18429/JACoW-SRF2023-WEPWB048

The rod radius is fixed at 12 mm to maintain sufficient cooling when the multipacting phenomena occur and to avoid microphonic vibration. The source of these vibrations is helium bubbles forming in the rods when the power dissipated is important, particularly for modes 2 and 3 [7]. Also, the higher radius of the rods allows their better cooling during multipacting. It has been proven that multipacting occurs around the pole shoes and coaxial gap [10].

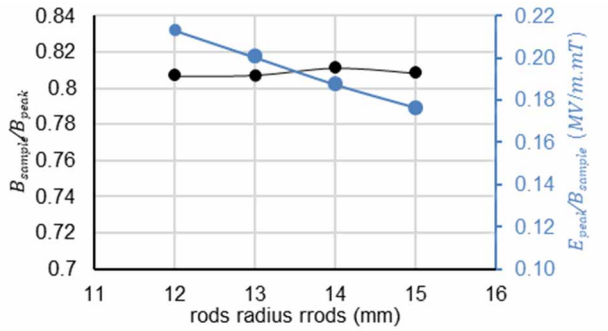

Figure 4: B_{sample}/B_{peak} and E_{peak}/B_{sample} vs. rods radius (rrods).

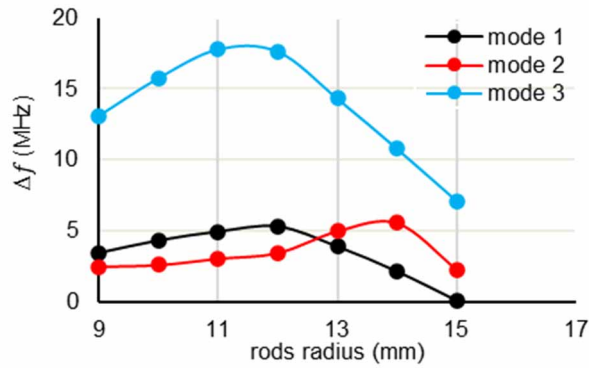

Figure 5: Measurement range Δf vs rods radius (r_{rods}) for three modes.

The focusing of the magnetic field on the sample depends strongly on the pole shoes size. The magnetic field profile at the sample follows the shape of the pole shoes, as shown in Fig. 6. To obtain accurate results in surface resistance with the calorimetric compensation method, the RF dissipation and the power loss from the heat should have the same profile on the sample and be more concentrated in the center. However, the concentration of RF power and E_{peak}/B_{sample} improves with values of lower values of r_{loop} and w_{loop} (see Figs. 7, 8). But increasing w_{loop} and r_{loop} improves the measuring range, field emission, and Δf (see Fig. 8, Fig. 9). For the JLab QPR, the r_{loop} was set to 5 mm.

RESULT AND DISCUSSION

After carrying out the individual parameter scans, a new model with several changes is implemented (see Table 2). The size of the pole shoes is similar to CERN's QPR 1. Table 3 lists the RF figure of the merits of the optimized

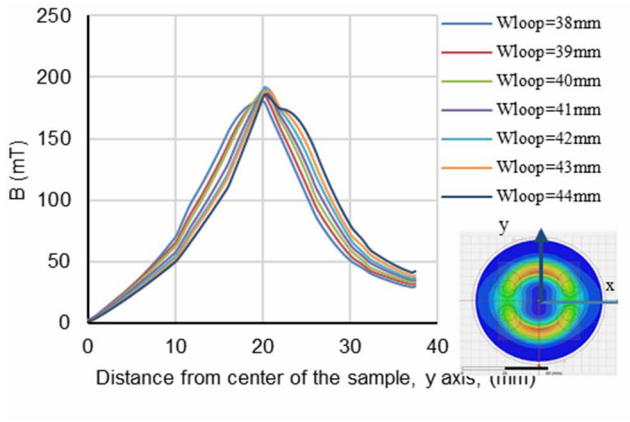

Figure 6: Magnetic field on the sample from the center to edge passing between half-pole shoes (y axis).

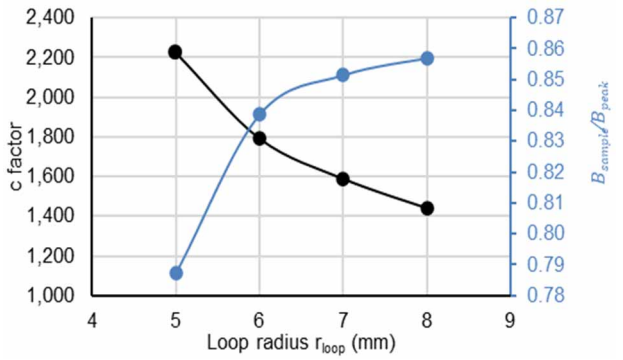

Figure 7: c factor and B_{sample}/B_{peak} vs. loop radius (rloop).

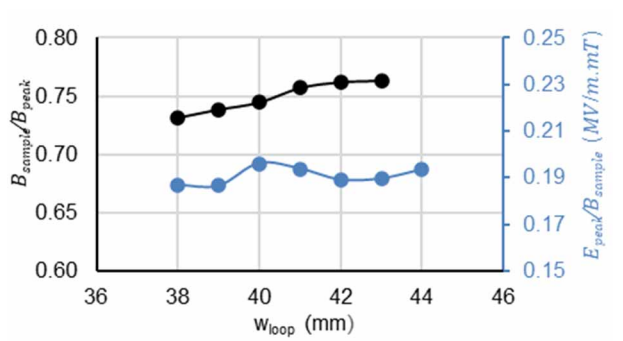

Figure 8: B_{sample}/B_{peak} and E_{peak}/B_{sample} vs. W_{loop}.

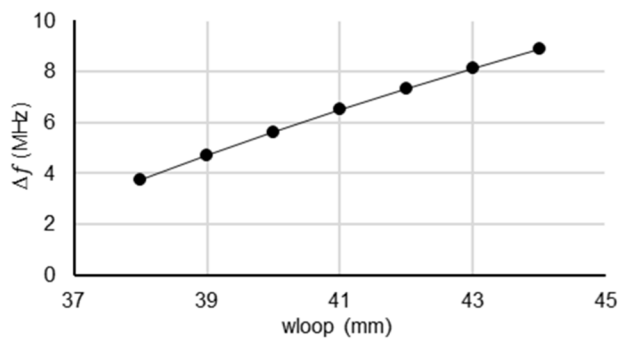

Figure 9: Measurement range Δf vs W_{loop} (mm).

ISBN: 978-3-95450-234-9 ISSN: 2673-5504 doi:10.18429/JACoW-SRF2023-WEPWB048

Table 2: Geometry of JLab QPR compared to CERN QPR 1 and 2

Parameter	CERN QPR1	CERN QPR2	JLab QPR
r_{rods}	8	15	12
h_{loop}	10	10	8
r_{loop}	5	8	5
w_{loop}	37.08	40.93	39
r_{coil}	20	23	20.89
d_{loop}	15	21	15
$L_{trans\ 1}$	15	16	15
$L_{trans\ 2}$	12.5	10	8

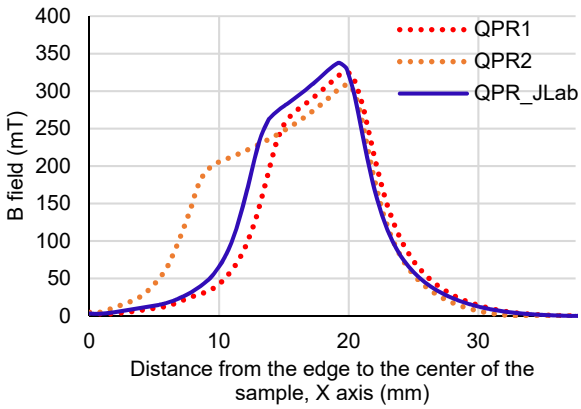

Figure 10: Magnetic field on the sample X axis.

design. We see that the result are similar to those of QPR 1. There is a significant improvement in the peak field ratio, particularly in increasing the surface magnetic field on the sample and decreasing the risk of field emission. The fields are more concentrated in the sample's center, allowing a higher resolution of the surface resistance measurement (see Fig.10). The quadrupole and dipole modes are separated Δf = 8.5 MHz. The microphonic simulation was performed which shows the first frequency vibration was ~105 Hz, which is safe microphonics level for QPR operation.

CONCLUSION

We have optimized the geometrical parameters for a new QPR via RF simulations for enhanced magnetic field distribution on the sample and removed potential overlapping modes. The QPR which will be used for R_s measurements of thin-film samples at JLab and it is being fabricated at CERN.

ACKNOWLEDGMENTS

We would like to thank QPR teams from DESY and HZB for providing helpful information and regular discussions.

Table 3: Comparison of RF Figures of Merit

Fields ratio	requirement	CERN QPR1	CERN QPR2	JLab QPR
Δf (MHz)	≥ 6	10.3	0.64	8.5
B_{sample}/B_{peak}	0.86	0.86	0.9	0.87
E_{peak}/B_{sample}	<0.25	0.25	0.2	0.19
B_{edge}/B_{sample}	< 0.1	0.07	0.12	0.06
c	>1000	1461	999	1422

REFERENCES

[1] R. L. Geng, G. V. Eremeev, Padamsee, H., and V. D. Shemelin, V. D., "High gradient studies for ILC with single-cell re-entrant shape and elliptical shape cavities made of fine-grain and large-grain niobium", in *Proc. Particle Accelerator Conference (PAC'07)*,Albuquerque, NM, USA, JUN. 2007, paper WEPMS0065, pp. 2337-2339.

[2] E. Mahner, S. Calatroni, E. Chiaveri, E. Haebel, and J. M. Tessier, "A new instrument to measure the surface resistance of superconducting samples at 400 MHz", *Rev. Sci. Instrum.,* vol. 74, no. 7, pp. 3390-3394, 2003. doi:10.1063/1.157857

[3] T. Junginger, W. Weingarten, and C. Welsch, "Extension of the measurement capabilities of the quadrupole resonator", *Rev. Sci. Instrum*., vol. 83, no. 6, p. 063902, 2012. doi:10:1063/1.4725521

[4] V. del Pozo Romano, R. Betemps, F. Gerigk, R. Illan Fiastre, and T. Mikkola, "Redesign of CERN's Quadrupole Resonator for Testing of Superconducting Samples", in *Proc. 18th Int. Conf. RF Superconductivity (SRF'17),* Lanzhou, China, Jul. 2017, pp.420-422. doi:10.18429/JACoW-SRF2017-TUPB016

[5] S. Aull, S. Doebert, T. Junginger, and J. Knobloch, "High resolution surface resistance studies", in *Proc. 6th Int. Conf. on RF Superconductivity (SRF'13),* Paris, France, Sep. 2013, paper WEIOC01, pp.785-788.

[6] R. Kleindienst, O. Kugeler, and J. Knobloch, "Development of an Optimized Quadrupole Resonator at HZB", in *Proc. 6th Int. Conf. on RF Superconductivity (SRF'13)*, Paris, France, Sep. 2013, paper TUP074, pp.608-610.

[7] T. Junginger, "Investigation of the Surface Resistance of Superconducting Materials", Ph.D. thesis, University of Heidelberg, Germany, 2012.

[8] S. Posen, N. Valles, and M. Liepe. "Radio frequency magnetic field limits of Nb and Nb 3 Sn." *Phys. Rev. Lett., vol.* 115, no. 4, pp. 047001-047005, 2015. doi:10.1103/PhysRevLett.115.047001

[9] P. Putek *et al*. "Shape optimization of quadrupole resonator for the RF characterization of superconductors," in *Proc. 22nd Int. Conf. on the Computation of Electromagnetic Fields, COMPUMAG'19*, Paris, France, Jun.-Jul. 2019, to be published.

[10] S. Bira *et al.*, "Multipacting Analysis of the Quadripolar Resonator (QPR) at HZB", in *Proc. SRF'21*, East Lansing, MI, USA, Jun.-Jul. 2021, pp. 42-45. doi:10.18429/JACoW-SRF2021-SUPCAV01